CrossMark

Original Paper

Production Decline Curves of Tight Oil Wells in Eagle Ford Shale

Henrik Wachtmeister,[1] Linnea Lund,[1] Kjell Aleklett,[1] and Mikael Höök [1,2]

This study derives typical production curves of tight oil wells based on monthly production data from multiple horizontal Eagle Ford shale oil wells. Well properties initial production (IP) rate and production decline rate were documented, and estimated ultimate recovery (EUR) was calculated using two empirical production decline curve models, the hyperbolic and the stretched exponential function. Individual well productivity, which can be described by IP level, production decline curvature and well lifetime, varies significantly. The average monthly IP was found to be around 500 bbl/day, which yields an EUR in the range of 150–290 kbbl depending on used curve, assumed well lifetime or production cutoff level. More detailed analyses on EUR can be made once longer time series are available. For more realistic modeling of multiple wells a probabilistic approach might be favorable to account for variety in well productivity. For less detailed modeling, for example conceptual regional bottom-up production modeling, the hyperbolic function with deterministic parameters might be preferred because of ease of use, for example with the average parameter values IP = 500 bbl/day, $D = 0.3$ and $b = 1$ resulting in an EUR of 250 kbbl with a 30-year well lifetime, however, with the recognition that this extrapolation is uncertain.

KEY WORDS: Tight oil, Shale oil, Well production, Decline rate, EUR, Eagle Ford.

INTRODUCTION

Extraction of oil and gas from shale formations has become a technically and economically viable complement to conventional oil production only within a decade. The great increase in shale oil production observed over the past couple of years, driven by high oil prices and new technology, was unforeseen by most analysts, and the initial estimates of potential production rates have already been surpassed in the USA (EIA 2008; IEA 2010). The development of horizontal drilling and advanced hydraulic fracturing (fracking) of shale formations has led to what has been described as a revolution in energy production in North America. Total US oil production has increased significantly (EIA 2014a), and shale oil now makes up almost half of total US oil production (EIA 2014b). The shale revolution in North America has been an eye-opener for the rest of the world regarding the possibilities for development of shale oil production. Analysts are now attempting to generate resource estimates for shale regions around the world and to project potential future production from these places, in the hope that the American shale revolution can be repeated elsewhere. So far, the most promising regions of technically recoverable resources outside of North America have been identified in Russia, China, Argentina and Libya (EIA 2013). However, some researchers also warn that recent estimates of contingent resources of shale oil and gas are too high (Hughes 2014; Inman 2014).

[1] Department of Earth Sciences, Uppsala University, Villavägen 16, 752 36 Uppsala, Sweden. URL: http://www.geo.uu.se
[2] To whom correspondence should be addressed; e-mail: mikael.hook@geo.uu.se

This study aims to increase the understanding of individual tight oil well production behavior, a key step in assessing overall production potential and recoverable resources of unconventional tight oil using bottom-up methods (where tight refers to the low permeability, typically ranging from nD to μD, of the oil-bearing rock). This was done by empirical analysis of monthly production data from multiple individual shale oil wells from the prolific Eagle Ford shale play in Texas. Decline curve analysis using two empirical models, the hyperbolic and the stretched exponential function, was used to derive typical tight oil production curves. Initial production (IP) rates were compiled, and together with derived production decline curves estimated ultimate recovery (EUR) of wells was calculated based on different assumptions of well lifetime. The overarching goal was to derive well-founded estimates for characteristic production behavior for a typical Eagle Ford well that could be useful for energy models using bottom-up approaches for future shale oil developments.

Understanding of individual well production potential and constraints is important for regional modeling, but also for environmental and economic analyses. For example, it could be used for linking material and labor need per well to necessary drilling activity in an area to uphold certain production levels. Increased understanding of tight oil production patterns and reasonable mean values that could be used in more multifaceted system models would be useful for energy planning and policy making.

METHODS AND DATA

Decline Curve Analysis

The characteristic production curves were derived by decline curve analysis. This methodology has been extensively used on conventional oil and gas wells for over a century to describe and predict production decline rate and EUR. An advantage is that less detailed data are required; however, the methodology is not as robust in long-term predictions as detailed geological modeling (McGlade et al. 2013). The exponential and hyperbolic curves, initially proposed by Arps (1945), are widely used for conventional oil wells. Other curves, like the hyperbolic curve describing nonconstant decline rates, have been suggested for horizontal and hydraulically fractured well. These include the

power-law exponential model (Ilk et al. 2008), stretched exponential model (Valkó 2009), logistic growth model (Clark et al. 2011), Duong model (Duong 2011) and scaling decline model (Patzek et al. 2013). All these curves, except the scaling decline model, are purely empirical and a posteriori justified by high goodness of fit and agreement with production data. Ideally, a derivation based on physics and geology should be desired in a model. Ease of use is also a desired quality.

The foundation of decline curve analysis is based on Arps (1945). The concepts of the loss-ratio $1/D$ and the derivative of the loss-ratio b are central in the definition of two empirical decline curves. The loss-ratio is defined as:

$$\frac{1}{D(t)} = -\frac{q(t)}{\mathrm{d}q(t)/\mathrm{d}t} \qquad (1)$$

where $D(t)$ is the decline parameter and $q(t)$ is the production rate. In the case of a constant loss-ratio (constant decline parameter), integration of Eq. 1 leads to an exponential decline curve:

$$q(t) = q_0\exp(-D(t - t_0)) \qquad (2)$$

where q_0 is the production rate at time t_0 (peak production or IP of the decline phase). Arps' (1945) derivation of the exponential decline curve was empirical, but it has later been shown to represent the solution to the physical flow equation of a homogeneous field with a given initial drive pressure that is reduced by extraction (Höök et al. 2014). Differentiating the loss-ratio leads to the following expression of the derivative of the loss-ratio b:

$$b(t) = \frac{\mathrm{d}}{\mathrm{d}t}\left[\frac{1}{D(t)}\right] = \frac{\mathrm{d}}{\mathrm{d}t}\left[-\frac{q(t)}{\mathrm{d}q(t)/\mathrm{d}t}\right] \qquad (3)$$

Assuming a constant derivative of the loss-ratio and integrating Eq. 3 lead to the expression of the hyperbolic decline curve:

$$q(t) = \frac{q_0}{[1 + D_0 b(t - t_0)]^{1/b}} \qquad (4)$$

where D_0 is the decline at time t_0 and $0 < b < 1$. The special case of $b = 0$ gives the exponential decline in Eq. 2, and the case of $b = 1$ gives what is called a harmonic decline. The harmonic decline model generates an infinite EUR, which is infeasible unless combined with some cutoff criterion. Fitting of hyperbolic curves to shale oil and gas production often leads to b values exceeding 1. This might be a result of very low reservoir permeability (Ilk and

Blasingame 2013), and yields an infinite EUR, like the harmonic decline model. Furthermore, hyperbolic decline is only valid during boundary-dominated flow and in shale gas wells flows may be transient for years or decades. Because of these shortcomings, attempts were made to find better representations of the production than the simplistic Arps curves. One way is simply to limit the hyperbolic curve in the long term by switching to an exponential curve at some point or to cut production at some suitable level.

Ilk et al. (2008) observed cases in shale gas production where the b parameter is not constant and highlights that hyperbolic curves are not suitable for a correct description. The function given by Eq. 5 is suggested to replace the constant decline parameter D (Ilk et al. 2008):

$$D(t) = D_\infty + D_1 t^{-(1-n)} \qquad (5)$$

where D_∞ is the decline constant at "*infinite time*," i.e., the dominating decline for large times given a purely exponential long-term decline, and D_1 is the decline constant "*intercept*" at 1 time unit and n is a time exponent. Inserting Eq. 5 into Eq. 1 and integrating give what we call the power-law loss-ratio decline:

$$q(t) = \hat{q}_i \exp\left(-D_\infty t - \frac{D_1}{n} t^n\right) = \hat{q}_i \exp\left(-D_\infty t - \widehat{D}_i t^n\right) \qquad (6)$$

where $\hat{q}_i$ is the "rate intercept" and differs from q_0 in the exponential and hyperbolic decline curves, which is simply the IP rate. The $\hat{q}_i$ is different from the IP, and a large $\hat{q}_i$ value compensates for a small n value.

A similar relation was independently suggested by Valkó (2009), with the only difference that long-term decline of D_∞ is omitted. This relation, called the stretched exponential decline model, is defined as:

$$q(t) = \hat{q}_i \exp\left(-\left(\frac{t}{\tau}\right)^n\right) = \hat{q}_i \exp\left(-\widehat{D}_i t^n\right) \qquad (7)$$

The stretched exponential decline curve can be expressed as an infinite sum of exponentials. The exponential decline curve represents the depletion-driven decline (Höök et al. 2014), but a fractured reservoir has not only the original pressure gradient from the reservoir but also an induced pressure from the fracturing fluid. For this reason, it can be expected that different pressure gradients will cause different decline regimes and that the total decline will be a sum of exponential declines derived from the different pressure gradients.

Patzek et al. (2013) derived a decline curve based on the physics of gas diffusion within the rock. The suggested scaling curve declines as one over the square root of time ($1/\sqrt{t}$) early on before it transits to exponential decline at a later stage. The wells produce at a rate of one over the square root of time as long as the initial pressure is kept in the reservoir. When the pressure drops below the original reservoir pressure the production rate decreases. This point is referred to as the interference time and can be found by plotting the square root of time versus the cumulative production. The point where this curve deviates from a straight line is the interference time. Eventually, the produced amount of gas is proportional to the remaining gas, which is the definition for the exponential decline.

Decline Curve Selection

The following criteria were considered for selection of which decline models to use in the study. First is a high goodness of fit and agreement with production data of the decline curve. Other criteria are a derivation based on physics and geology and the ease of use. Another aspect to take into account is the number of estimated parameters in the model. The number of data points should be at least 10 times the number of estimated parameter to make good fits and avoid overfitting (Höök 2014). Since the data series available in this study are quite limited in time, the use of fewer parameters was preferred.

The model of oil production with the strongest connection to the geology is the scaling decline model. The difficulty in determining the interference point of individual oil wells complicates the use of the scaling decline curve, and for this reason, it was not used in this study. The power-law loss-ratio decline curve and the stretched exponential decline curve are similar, but the former has been shown to better model long-term production (Ilk et al. 2008). However, the latter has one less parameter to estimate and is therefore easier to use with less risk of overfitting. The Arps' exponential and hyperbolic decline curves have long been shown to give a good agreement to empirical data. Another advantage of the Arps curves is their ease of use. For shale oil production, the exponential curve is not sufficiently flexible, but the hyperbolic curve has the potential to model shale oil production well.

Table 1. Some important properties of the hyperbolic and the stretched exponential decline curves

	Hyperbolic	Stretched exponential
$q(t)$	$q_0[1 + D_0 b(t - t_0)]^{-1/b}$	$\hat{q}_i \exp\left(-\widehat{D}_i t^n\right)$
$Q(t)$	$Q_0 + \frac{q_0}{D_0(1-b)}\left[1 - \left(1 + D_0 b(t-t_0)^{1-1/b}\right)\right]$	$Q_0 + \frac{\hat{q}_i \tau}{n}\left\{\Gamma\left[\frac{1}{n}\right] - \Gamma\left[\frac{1}{n}, \left(\frac{t}{\tau}\right)^n\right]\right\}$
EUR	$Q_0 + (q_0/D_0(1-b))$	

The two decline models that were used in this study are the hyperbolic and the stretched exponential decline curves. The advantages of these decline curves lie in their strong empirical compliance and ease of use. Some important properties of the hyperbolic and the stretched exponential curves are expressed in Table 1, from Valkó (2009), Höök et al. (2014), Satter et al. (2008) and Kanfar (2013). $Q(t)$ is the cumulative production at time t, and EUR is the estimated ultimate recovery of the well. In the cumulative production of the stretched exponential curve, the first term inside the brackets is the complete gamma function and the second term is the incomplete gamma function. From Eq. 7, τ is equal to $\left(1/\widehat{D}_i\right)^{1/n}$.

Data Considerations

The production data used originate from the proprietary database Drillinginfo (2014). This database provides estimates of monthly production data (and many other parameters) for individual wells. The Eagle Ford data provided by Drillinginfo are based in turn on the Texas Railroad Commission (RRC) database, which contains monthly production figures per lease, not per individual wells. In reality, what constitutes an individual well is convoluted and can change with time. Also, since a lease can contain several ''wells,'' estimations from RCC data must be made. Drillinginfo's definition and implicit estimation of a ''well'' were used throughout this study. In particular, ''tight oil wells'' are identified using the definition of a horizontal well that is classified as oil well only (in contrast to gas wells). For production volume data, Drillinginfo's definition of oil was used, which includes condensate but not gas. The production figures are in unit barrels (bbl) of oil (in contrast to oil and gas reported in unit barrels of oil equivalents).

The time frame of the data set used in this study spans from January 2010 through September 2014. A total of 6663 horizontally drilled wells are re-

ported in the Eagle Ford reservoir for this time period. Only a smaller subset (35% or 2312) of these wells' has production data that are usable in this analysis due to the way production is reported in the Drillinginfo database. The production patterns sought in this study are those generated for a single well by the prevailing physical conditions, such as the size of the reservoir, the geology of the rock and the physical flow constraints. When production is reported as a sum of several wells with different starting points in time, the corresponding production decline patterns of individual wells become obfuscated. Hence, such combined well production time series was excluded. The share of the wells that are reported individually has increased from year to year from 14% in 2010 to 18% (2011), 28% (2012), 49% (2013) and 63% (2014). Before analysis, months with zero production were removed to exclude external events such as annual maintenance and scheduled downtime that affected production.

Goodness of Fit

Curve fits should be discarded unless they are capable of describing well behavior in a statistically acceptable way that agrees with actual data. This is referred to as the goodness of fit and can be measured in several ways.

Two measures of goodness of fit were used in this study. The first measure is the coefficient of determination, R^2, defined as one minus the residual sum of squares over the total sum of squares (Upton and Cook 2008):

$$R^2 = 1 - \frac{\text{Sum of squares of residuals}}{\text{Total sum of squares}}$$
$$= 1 - \frac{\sum_i (y_i - \hat{y}_i)^2}{\sum_i (y_i - \bar{y})^2} \tag{8}$$

where y represents observed data points, $\hat{y}$ represents values predicted by the model, and $\bar{y}$ is the mean of the observed data. The R^2 ideally has a value between 0

and 1 and illustrates how well the observed data are explained by a chosen model. Values of R^2 outside the range 0–1 can occur where it is used to measure the agreement between observed and modeled values and where the "modeled" values are not obtained by linear regression and depending on which formulation of R^2 was used. The description gets increasingly more accurate as R^2 becomes closer to 1.

The second measure of goodness of fit that was used is the root-mean-square error, RMSE, which is defined as the square root of the squared residuals divided by the residual degrees of freedom (Upton and Cook 2008):

$$\text{RMSE} = \sqrt{\frac{\sum_i (\hat{y}_i - y_i)^2}{n - m}}$$

where n is the number of data points and m is the number of estimated coefficients.

Nonlinear least square methods were used to fit data to the mathematical models, using the trust region algorithm (Byrd et al. 1987). Poor curve fits were excluded based on goodness of fit boundaries described in the next section.

Aggregate Well and Individual Well Type Curves

In this study, two separate approaches were used for examining the decline in shale oil wells. First, the "*aggregate wells decline*" was studied. The "*aggregate wells decline curve*" is a decline curve that is fitted to the average production curve of several wells. The advantage of this average curve of monthly production is that fluctuations are smoothed out. The longer the production time series, the better the identification of long-term productivity. However, wells with long production data series are few. For this reason, different numbers of wells were used for different segments of the curve. Only wells with cumulative production exceeding 20 kbbl were included since wells with less cumulative production were regarded as unsuccessful and would disturb the production patterns of successful

ones. This implies rejection of 387 (or ~17%) of the 2312 individually reported wells.

Secondly, individual well decline curves were studied. The hyperbolic curve and the stretched exponential curve were fitted to the production data from individual wells. The wells with poor fits were excluded because the estimated parameters of these curve fits have little accuracy. The boundaries that were introduced to exclude the poorest fits are $R^2 > 0.75$ and RMSE < 0.1. These limits are quite permissive, and the fits that meet the conditions are not necessarily exceptionally good fits, but the measure was used to exclude very poor fits.

There is a trade-off between the number of wells included and the number of data points (number of months). To avoid overfitting, the number of observed data points should be at least 10 times the estimated parameters (Höök 2014). Consequently, the appropriate minimum number of production month data was 20 for the hyperbolic curve and 30 for the stretched exponential curve. Only 9% of the 2312 individually reported wells have production data exceeding 30 months, and for this reason wells with production data exceeding 25 months were included as a compromise between number of wells included and the number of data points per fitting parameter. These wells represent 15% of all wells, and after excluding poor fits only 13% of the 2312 wells remain. Consequently, only wells from 2010, 2011 and early 2012 can be included in this analysis. No obvious reason can be seen for why the analyzed wells should not be fairly representative of the whole when constraints imposed by the analytical methodology and the way well data are reported by Drillinginfo are acknowledged.

RESULTS

Annual Decline Rates

An initial derivation of simple empirical annual decline rates during the first 3 years was made before fitting decline curves to production data. The average annual decline rates presented in Table 2

Table 2. Mean annual decline rate during first, second and third year of production

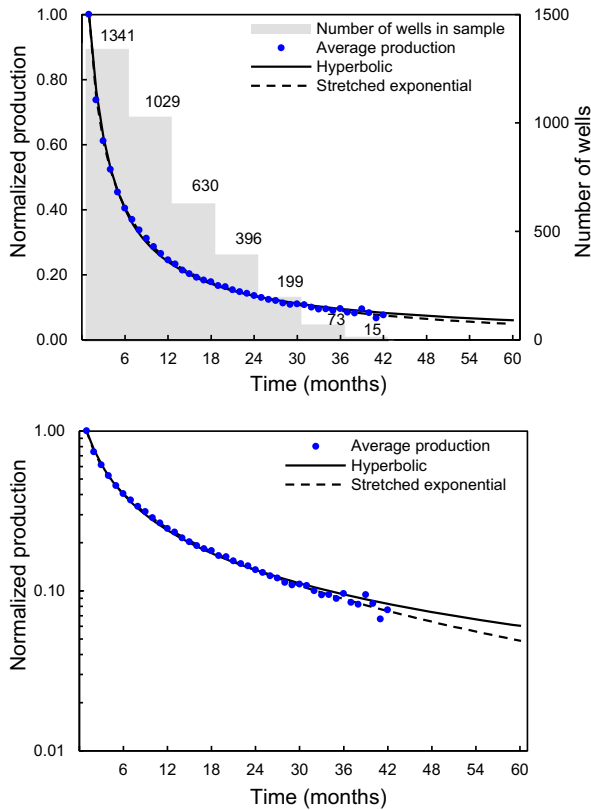|	Year 1 (%)	Year 2 (%)	Year 3 (%)
Mean annual decline rate (%)	74	47	19
Remaining production level (% of IP)	26	13	11

Figure 1. The hyperbolic and the stretched exponential decline curves fitted to average production data.

are based on the mean annual production decline rate of all wells with 12, 24 and 36 months of production, respectively. As seen, the decline rate is high the first year, 74%, and gradually decreases to 47 and 19% during the second and third years. As a result, remaining production as share of the well's IP is only 26% at the end of the first year. After 3 years only 11% of the IP level remains. Since there is no constant decline rate for tight oil wells, it is not recommended to represent the production with single exponential decline curve, as commonly done for production from conventional oil wells and fields (Höök 2014; Höök et al. 2014; Satter et al. 2008).

Instead, the production should be represented by models capable of relaying a changing decline rate over time such as the hyperbolic and stretched exponential decline curves.

Aggregate Well Decline Curve

Figure 1 shows the average production, derived by calculating the mean production of several wells, together with the hyperbolic and the stretched exponential best fits to this data. The curves are similar and hard to visually distinguish on a regular scale (top); for this reason the curves are also presented on a logarithmic scale (bottom). The number of wells that the average is based upon for the different sections is also included in the bottom figure.

The parameter values of the best fits are presented in Table 3. Both curves are good fits in terms of R^2 and RMSE. On the logarithmic scale, the two curves appear more different, but the cumulative production of the first 10 years of the stretched exponential curve is only 7.7% less than the cumulative production of the hyperbolic curve for the same period.

Individual Well Decline Curves

Hyperbolic Decline Curve

The production data from 294 wells that meet the requirements were used to fit hyperbolic decline curves from Eq. 4. Figure 2 shows the distribution of the b parameter of the hyperbolic fits. The probability distributions that best describe the b values according to χ^2 tests are the log-logistic distribution followed by a normal distribution (Fig. 2). A b value >1 is almost as common as a b value <1. Figure 3 shows the distribution of the D parameter. Also, a log-logistic distribution describes the estimated D

Table 3. Parameter values of best fits to aggregate well production data

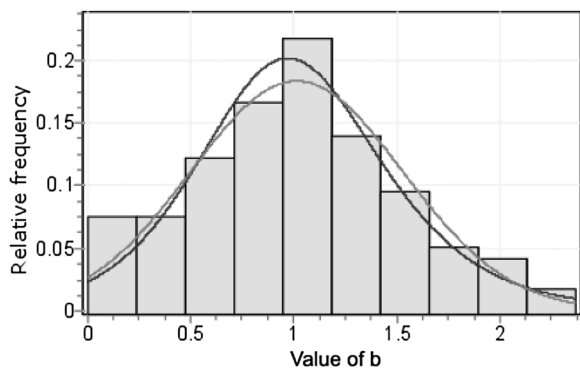|	D	b	R^2	RMSE
Hyperbolic	0.309	1.08	0.9984	0.0078
	$\hat{q}_i$	$\widehat{D}_i$	n	R^2	RMSE
Stretched exponential	3.69	1.31	0.292	0.9996	0.0040

Figure 2. Distribution of the b parameter values of the hyperbolic decline curve fitted to individual production data of 294 wells (relative frequency histogram). The log-logistic distribution function (black) and the normal distribution (gray) may be used to describe the distribution of the estimated b parameter values.
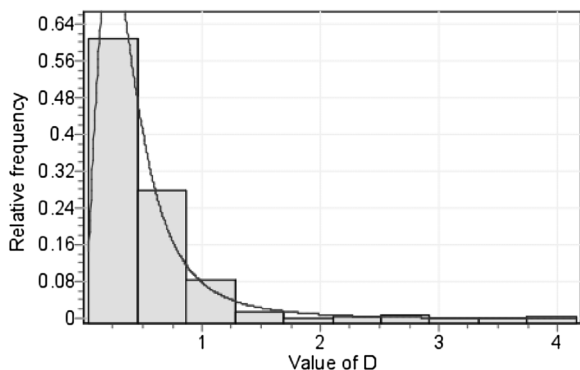

Figure 3. Distribution of the D parameter values of the hyperbolic decline curve fitted to individual production data of 294 wells. The log-logistic distribution function may be used to describe the distribution of the estimated D parameter values. D values are on the x-axis, and the probability function is on the y-axis (relative frequency histogram).

values in this case according to χ^2 tests. The mean, standard deviation and median value of the b and D distributions are presented in Table 4.

Stretched Exponential Decline Curve

The stretched exponential curve in Eq. 7 was fitted to production data from the 294 wells meeting the requirements. Some descriptive statistics of the estimated parameters are shown in Table 5. The parameter with the largest range is $\hat{q}_i$, ranging from below 1 to 7484. The three parameter estimates are interdependent, and a high value of $\hat{q}_i$ compensates

Table 4. Mean, standard deviation and median values of the D and b distributions of 294 individual wells

	D	b
Mean	0.488	1.10
SD	0.433	0.514
Median	0.369	1.00

Table 5. Descriptive statistics of the stretched exponential curve parameters of individual wells' production fits

	$\hat{q}_i$	$\widehat{D}_i$	n
Mean	482	3.01	0.352
SD	1130	2.83	0.293
Min	0.869	0.0146	0.0654
25% (Q1)	1.86	0.601	0.107
50% (median)	5.66	1.71	0.272
75% (Q3)	386	5.97	0.506
Max	7480	9.01	1.74

for a low values of n. $\hat{D}_i$ has a moderately strong correlation to both $\hat{q}_i$ (0.72) and n (−0.75), while the correlation between $\hat{q}_i$ and n is weaker (−0.38).

Summary and Comparison of Well Decline Curves

In Figure 4, production decline curves based on both aggregate and individual well production data are presented together. From the aggregate well data, the best fits from Figure 1 are shown. From the individual well data, the curves resulting from the median of the estimated parameters for the hyperbolic and stretched exponential curves are presented. As seen, the two stretched exponential curves decline faster than the two hyperbolic curves. Extrapolations based on aggregate data yield
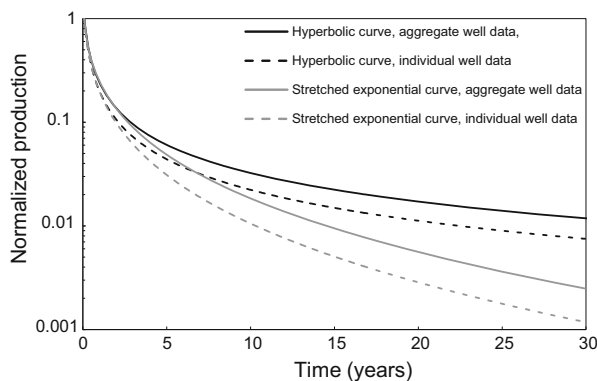

Figure 4. Hyperbolic and stretched exponential decline curves based on aggregate and individual well data.

somewhat higher production rates for both functions compared to extrapolations based on the median of individual well data.

Comparison by means of goodness of fit indicates that, based on the individual well results, a hyperbolic curve fit is better than the stretched exponential for 80% of the wells according to the RMSE and for 67% of the wells according to the R^2.

Variations in Initial Production

The peak production is typically reached within 1 or 2 months after the first production month in most wells, and it characteristically marks the onset of a decline phase. Therefore, the peak production will hereafter be referred to as IP. Accordingly, IP is the average production (e.g., expressed in barrels per day) of the month with the highest monthly production. Only a smaller part of the total yield is produced before the maximal production is reached, and most of the cumulative production over a wells lifetime comes from the decline phase. For this data set, the average pre-peak production is around 11% of the first-year total production.

Figure 5 shows the development of IP over time. The largest increase in mean IP is seen from 2010 to 2011, an increase of almost 30%, and smaller increases are seen for 2011–2012 and for 2013–2014. The number of wells included is shown on the secondary axis by the shaded bars. For 2014, data cover only the first 9 months, which partly explains the
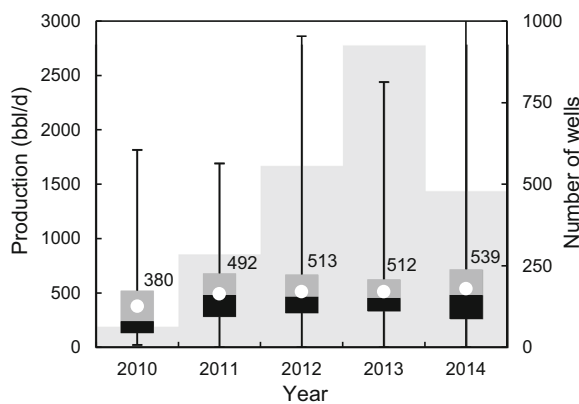

Figure 6. Distribution of the initial production in the 926 wells starting in 2013 with a fitted log-logistic probability distribution (relative frequency histogram).
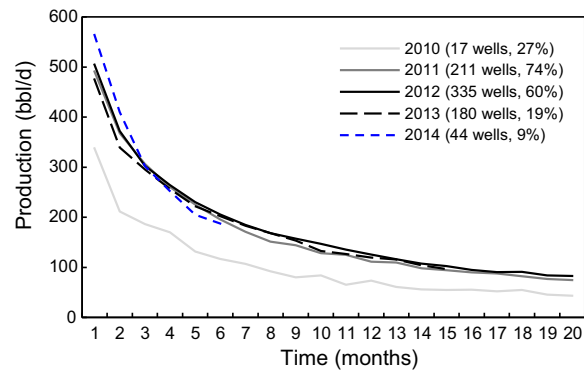
Figure 7. Production decline over the first 20 months for wells starting in year 2010, 2011, 2012, 2013 and 2014.

smaller sample. The 2014 average can be considered a preliminary estimate, which can be subject to adjustments in future studies since it was not based on a full set of 12 months.

Figure 6 shows an example of the distribution of the IP for 1 year, 2013. This is the year with the largest sample. The log-logistic probability distributions and other positively skewed distributions describe the IP well (skewness is 1.9).

Figure 7 shows average production for the first 20 months for wells starting in 2010, 2011 and 2012 and average production for the first 15 and 6 months for wells starting in 2013 and 2014, respectively. The average production in wells from 2011 to 2013 is similar. The average of 2014 wells is initially higher than the wells from previous years, in line with result from Figure 5. However, after a couple of months average production for 2014 is more similar to that of the wells of previous years or even lower. The

Figure 5. Boxplots of initial production (left axis) bar chart of well sample size (right axis) by year. A box presents lower quartile, median and upper quartile, and the whisker presents range, and also the mean value is presented with dot and quantity.
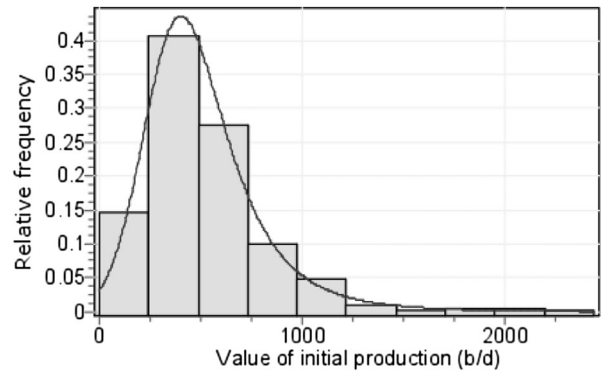
Table 6. Summary of initial production estimates from this and other studies

References		2010		2011		2012		2013		2014
Rystad Energy (2014)		265		385		445		480		495
This study (mean)		380		492		513		512		539

References	Atascosa	DeWitt	Dimmit	Gonzales	Karnes	LaSalle	Live Oak	Maverick	McMullen	Webb	Frio
Maugeri (2013)	276	709	244	443	471	171	565	84.4	308	173	–
Nysveen (2014)	500	670	375	750	700	400	400	–	450	175	350
Hughes (2014)	300	475	200	510	500	250	345	–	300	140	–

Initial oil production is expressed in bbl/day, derived as the average during the first month of production

Table 7. Different estimated ultimate recovery (EUR) of an average Eagle Ford well based on different decline curves and well lifetimes

	EUR based on assumed well lifetime (kbbl)						EUR based on 4 bbl/day cutoff	
	5 years	10 years	15 years	20 years	25 years	30 years	Cutoff year	EUR (kbbl)
Aggregate wells								
Hyperbolic (best fit D and b)	151	192	217	235	249	261	46	290
Stretched exponential (best fit $\hat{q}_i$, $\widehat{D}_i$ and n)	162	190	203	209	214	216	17	205
Individual wells								
Hyperbolic (median D and b)	125	153	170	182	192	199	29	198
Stretched exponential (median $\hat{q}_i$, $\widehat{D}_i$ and n)	132	149	156	160	162	163	12	153

numbers of wells that the annual averages are based on are included in the legend along with the share of the total of new wells that they represent. As seen, the data for 2011 and 2012 cover a relatively large share of all wells. On the other hand, samples for 2010, 2013 and 2014 cover a smaller share and should be handled with more caution.

In Table 6, IP numbers for Eagle Ford from other studies are summarized. Variations both between counties and studies can be seen. What is usually referred to as IP is the average production over the first 30 days, which is also what is defined as IP in other studies (Maugeri 2013; Nysveen 2014; Rystad Energy 2014). In this study, only monthly production data are available and consequently the first 30-day production cannot be distinguished from the data. Instead, the IP is calculated as the average daily production of the month with the highest production. It is unclear how the IP is defined in Hughes (2014).

Well Lifetime and Estimated Ultimate Recovery

As of 2014, the earliest horizontal and hydraulically fractured wells in the Eagle Ford have not yet been producing for more than 4 years.

Thus, it is premature to determine well lifetime solely from historical production data. A large share of the wells, 24%, that started in 2010–2012 has not had any reported production after March 2014. Closer analysis indicates that most of these wells have not been terminated, but rather their reported production is bundled with other wells after a few months' production. Hence, such wells cannot be used for analysis whether they have been successful or not.

Kaiser and Yu (2010) studied the economic limits of field production in Texas between 1993 and 2008. The final annual average production in all land wells is ~5 barrels of oil equivalents per day (boe/d). A 20% efficiency gains are simplistically assumed to account for future improvements, and this gives a usable cutoff criteria at an average annual production level of 4 bbl/day.

An average Eagle Ford well with corresponding range of EUR can be constructed by applying the four decline curves from Figure 4, using the 2010–2014 mean IP of 512 bbl/day and applying a cutoff rate of 4 bbl/day results in the EUR figures shown in Table 7 under ''EUR based on 4 bbl/day cutoff.'' The production curves and the cutoff rate are presented in Figure 8. In Figure 9, the cumulative production of the same curves is also presented.
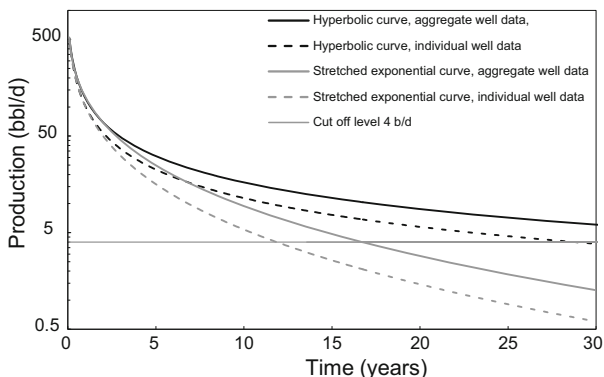
Figure 8. Extrapolations of hyperbolic and stretched exponential decline curves used to derive different well EUR.
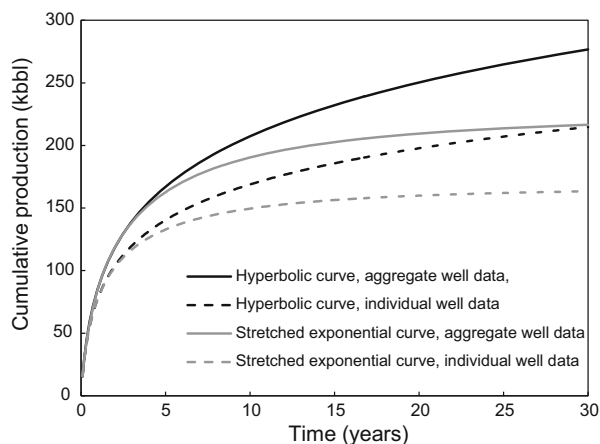

Figure 9. Cumulative production of decline curves used to derive different well EUR.

The different decline curves result in well lifetimes between 12 and 46 years and a total production of 153–290 kbbl when applying the cutoff criteria. In Table 7 cumulative production from the same decline curves is also presented for different time periods. The mean production during the time before peak production (which this study uses as IP)

month is 13 kbbl, which represent 4–6% of different EUR estimates. This estimate of 13 kbbl could be added to the EUR figures in Table 7 if deemed appropriate.

Finally, Table 8 shows the EUR from other similar studies focused on average wells in the Eagle Ford for comparison. EIA (2014b) and Swindell (2012) report somewhat lower EUR values than this study. Differences can likely be explained by differences in underlying data sets and EUR calculation methods, such as extrapolation method and well lifetime or cutoff criteria.

DISCUSSION

Both the hyperbolic and the stretched exponential function fit well to average production data and to data from individual wells in the Eagle Ford. The hyperbolic curve gives a better fit in most cases according to the R^2 and the RMSE measures. However, it is a significant deficit that the data series are short and, resultantly, long-term production behavior is not adequately covered. The two alternative decline curves are very similar for the first 3 years, and the difference between the two become significant only at the very end of the available production series. Longer production data series are required to find out which curve is better in the long term.

There is a risk of overestimating production when using a hyperbolic curve. The hyperbolic curve with the b parameter greater than one cannot solely be used to predict the total production from a well since it will generate an infinite resource. Hence, the hyperbolic curve may describe production well for a limited period of time and could be used for predicting production as long as one is aware that it cannot be extrapolated into infinity. This can be handled by truncating the curve at some point, such

Table 8. Estimated ultimate recovery (EUR) of an average Eagle Ford well according to other studies using decline curve analysis

References	EUR (kbbl)	Type of estimate	Method	Well life	Well data
EIA (2014a, b)	168	Mean of individual wells' EUR	Hyperbolic decline curve fitted to individual wells with ≥4-month data, shifts to exponential decline when 10%	30 years	2008–2013
Swindell (2012)	115	Mean of individual wells' EUR	Hyperbolic decline fitted to individual wells where ''decline rate sufficiently established''	Economic	2008–2012
Hughes (2014)	296	EUR of aggregate average well	Average aggregate well decline profile for first 4 years, then assumed exponential decline rate of 15%	25 years	2009–2014 May

as cutoff production rate or applying a given lifetime as done here. EIA (2014b), Hughes (2014) and others have resolved that by shifting to exponential decline at some point.

In comparison, the stretched exponential decline curve is advantageous as production declines to zero and the risk of calculating unrealistically large EUR estimates is reduced. The aggregate decline curves and the average of the individual well decline curves differ from each other when generating a range of possible long-term production trajectories.

Production of tight oil wells declines fast, on average 74, 47 and 19% annually for the first, second and third year of production, respectively, based on data from the Eagle Ford formation. These numbers broadly agree with Hughes (2014), study on Eagle Ford (first year 62, second year 32 and third year 18%) and Bakken (72 first year, 34 s year, 22% third year). Hughes (2014) has a similar data set, as he also used data from Drillinginfo (2014). The discrepancy is likely a result of underlying differences in what wells that were included.

The observed development of annual mean IP shows two relatively larger increases, from 2010 to 2011 and from 2013 to 2014. These increases could be the result of newly defined sweet spots since shale oil extraction in the Eagle Ford is still at a quite early stage. Also, the increases could be a result of advances in technology such as increased horizontal lengths of wells and increased number of fracturing stages. However, it is hard to distinguish a clear trend in the development of IP (Fig. 5). An uncertainty in the development of IP also comes with the selection of wells that can be included in analysis. For 2010 and 2011, less than 20% of all wells have individually reported production and there is a larger uncertainty in assuming that these wells represent all wells' behavior well than if a larger share of the wells had been included in the analysis. Rystad (Rystad Energy 2014) observes a similar development in IP as found in this study, but at somewhat lower production levels. An explanation could be the difference in measuring/calculating IP. The Rystad values are the averages over the first 30 days of production, while in this study the values are based on the month with highest production, which should result in higher values if the month of maximum production is not the first month.

This study did not venture deeper into exploring the cause of differences in IP seen for counties identified by other studies (Maugeri 2013; Hughes 2014; Nysveen 2014). However, plausible explanations include the location of sweet spots in the Eagle Ford shale play as well as different operator strategies. Another possible factor could be the API gravity of the oil that differs from county to county. This has been discussed by Gong (2013).

The well EUR estimates derived here have intrinsic shortcomings due to the length of available data series. Only longer production time series will reduce this uncertainty and provide improved and more appropriate evidence for decline curve model and assumed well lifetime. It is encouraged that a similar study should be undertaken once longer time series are available. However, the following can be noted. Hyperbolic curve gives higher EUR than stretched exponential based on the same data. This can be expected since stretched exponential allows for nonconstant decline rate in the longer term, while hyperbolic decline rate can settle at a low level. Also, extrapolations based on aggregate well data give higher EUR than based on median of individual well data for both curves. The aggregate well time series consist of 42 data points. The individual well time series vary from 25 to 42 data points. Generally, it is seen that decline rates decrease with time. Therefore, it is possible that the aggregate well data with its longer time series "steer" the extrapolation to a trajectory with lower decline rate, compared to extrapolations based on shorter underlying time series.

Assuming a cutoff rate at a 12-month average production of 4 bbl/day, all decline curves yield EUR values in the range 153–290 kbbl for a typical Eagle Ford well. This range includes the estimates derived reported by EIA (2014b) and Hughes (2014) (Table 8). The EIA used 5667 wells with more than 4-month production and fits hyperbolic decline curves to the monthly production data. However, a data series with only 4-month data has major shortfalls when subjected to curve fitting for 30-year well lifetimes and likely contribute to the lower EUR estimates. Hughes (2014) used a data set of 10,088 wells, but it is unclear which of these wells were included in the decline analysis that provides the basis of the EUR estimates. Swindell (2012) used a smaller data set with just over 1000 wells—the available data in 2012. Conceivable explanations for the differences between Swindell and this study may thus be due to the longer data sets available, differences in decline rates and technological advances in drilling and fracturing.

When it comes to future production from the entire Eagle Ford shale play, parameters such as well spacing, drilling activity, social acceptance and

oil price are important along with the decline rates in individual wells. These parameters have not been investigated in this paper but should be examined in further studies with a more holistic system approach to shale oil and its exploitation for supplying society with useful energy.

CONCLUSIONS

Production of tight oil wells declines fast, on average 74, 47 and 19% annually for the first, second and third year of production, respectively, based on investigated data from the Eagle Ford formation. These numbers broadly agree with Hughes (2014), study on Eagle Ford and Bakken. Hyperbolic and stretched exponential curve fit models can be used to model this production behavior.

Individual well productivity varies significantly and can be described by IP level, production decline curvature and well lifetime. The distribution of wells' IP level is positively skewed with a mean of 512 bbl/day. Average IP level increased in early years of Eagle Ford development but has slowed down since 2011.

Extrapolation of representative average production curves yields EUR of tight oil wells in the range of 153–290 kbbl depending on used curve, assumed well lifetime or production cutoff level (Table 7). This generally agrees with earlier studies using decline curve analysis (Table 8), but this kind of extrapolation-derived EURs is uncertain. More detailed analyses on EUR should be made once longer time series are available.

For more realistic modeling of multiple wells, a probabilistic approach might be favorable to account for the large variety in individual well productivity. For less detailed modeling, such as more conceptual regional bottom-up modeling, the hyperbolic function with deterministic parameters might be preferred because of ease of use and familiarity. For example, the average parameter values IP = 500 bbl/day, $D = 0.3$ and $b = 1$ resulting in a EUR of 250 kbbl with a 30-years well lifetime could be used as a reasonable assumption, with the recognition of the uncertainties involved. Accordingly, due to the relativity low EUR per well, any high regional production estimate requires a high estimate of well drilling.

OPEN ACCESS

REFERENCES

Arps, J. J. (1945). Analysis of decline curves. *Transactions of the AIME, 160,* 228–247.

Byrd, R. H., Schnabel, R. B., & Shultz, G. A. (1987). A trust region algorithm for nonlinearly constrained optimization. *SIAM Journal on Numerical Analysis, 24,* 1152–1170.

Clark, A. J., Lake, L. W., & Patzek, T. W. (2011). Production forecast with logistic growth models. In *Presented at the SPE annual technical conference and exhibition.* Society of Petroleum Engineers, Denver, CO, USA.

Drillinginfo. (2014). Drillinginfo database. Retrieved December 2016 from http://drillinginfo.com/.

Duong, A. N. (2011). Rate-decline analysis for fracture-dominated shale reservoirs. *SPE Reservoir Evaluation and Engineering, 14,* 377–387.

EIA. (2008). Annual energy outlook 2008 (No. DOE/EIA-0383(2008)). Washington, DC: Office of Integrated and International Energy Analysis, U.S. Energy Information Administration (EIA), U.S. Department of Energy.

EIA. (2013). Technically recoverable shale oil and shale gas resources: An assessment of 137 shale formations in 41 countries outside the United States. Washington, DC: U.S. Energy Information Administration (EIA), U.S. Department of Energy.

EIA. (2014a). Petroleum and other liquids: Crude oil production. Retrieved December 2016 from http://www.eia.gov/dnav/pet/pet_crd_crpdn_adc_mbbl_m.htm.

EIA. (2014b). Annual energy outlook 2014 (Report No. DOE/EIA-0383(2014)). Washington, DC: Office of Integrated and International Energy Analysis, U.S. Energy Information Administration (EIA), U.S. Department of Energy.

Gong, X. (2013). *Assessment of Eagle Ford shale oil and gas resources.* Doctoral dissertation, Texas A & M University.

Retrieved December 2016 from http://hdl.handle.net/1969.1/151324.

Höök, M. (2014). Depletion rate analysis of fields and regions: A methodological foundation. *Fuel, 121,* 95–108.

Höök, M., Davidsson, S., Johansson, S., & Tang, X. (2014). Decline and depletion rates of oil production: A comprehensive investigation. *Philosophical Transactions of the Royal Society A, 372,* 20120448.

Hughes, J. D. (2014). *Drilling deeper.* Report from Post Carbon Institute. Retrieved December 2016 from http://www.postcarbon.org/publications/drillingdeeper/.

IEA. (2010). World energy outlook 2010. Paris: International Energy Agency (IEA), Organisation for Economic Co-operation and Development.

Ilk, D., & Blasingame, T. A. (2013). Decline curve analysis for unconventional reservoir systems—Variable Pressure Drop Case. In *Presented at the SPE unconventional resources conference.* Society of Petroleum Engineers, Calgary, AB, Canada.

Ilk, D., Rushing, J. A., Perego, A. D., & Blasingame, T. A. (2008). Exponential vs. hyperbolic decline in tight gas sands. In *Presented at the SPE annual technical conference and exhibition.* Society of Petroleum Engineers, Denver, CO, USA.

Inman, M. (2014). Natural gas: The fracking fallacy. *Nature, 516,* 28–30.

Kaiser, M. J., & Yu, Y. (2010). Economic limit of field production in Texas. *Applied Energy, 87,* 3235–3254.

Kanfar, M. S. A. (2013). Comparison of empirical decline curve analysis for shale wells. Master's thesis, Texas A & M University. Retrieved December 2016 from http://hdl.handle.net/1969.1/151124.

Maugeri, L. (2013). The shale oil boom: A U.S. Phenomenon (No. 2013–05 Discussion Paper). Cambridge: Belfer Center for Science and International Affairs.

McGlade, C., Speirs, J., & Sorrell, S. (2013). Methods of estimating shale gas resources—comparison, evaluation and implications. *Energy*, *59*, 116–125.

Nysveen, P. M. (2014). Eagle Ford update: EOG resources remains largest acreage holder. *Oil and Gas Financial Journal*, *11*(9), 63.

Patzek, T. W., Male, F., & Marder, M. (2013). From the cover: Cozzarelli Prize Winner: Gas production in the Barnett Shale obeys a simple scaling theory. *Proceedings of National Academy of Sciences, 110,* 19731–19736.

Rystad Energy. (2014). *US Shale newsletter* (Vol. 1 No. 3). Retrieved December 2016 from http://www.rystadenergy.com/NewsEvents/Newsletters/UsArchive/us-q3-2014.

Satter, A., Iqbal, G. M., & Buchwalter, J. L. (2008). *Practical enhanced reservoir engineering.* Tulsa: PennWell Corporation.

Swindell, G. S. (2012). Eagle Ford shale—An early look at ultimate recovery. In *Presented at the SPE annual technical conference and exhibition.* Society of Petroleum Engineers, San Antonio, TX, USA.

Upton, G., & Cook, I. (2008). *A dictionary of statistics* (2 rev ed.). New York: Oxford University Press.

Valkó, P. P. (2009). Assigning value to stimulation in the Barnett shale: A simultaneous analysis of 7000 plus production histories and well completion records. In *Presented at the SPE hydraulic fracturing technology conference.* College Station, TX, USA.